Minimum Time Bilateral Observer Design for 2×2 Linear Hyperbolic Systems

Nils Christian A. Wilhelmsen, Henrik Anfinsen, Ole Morten Aamo

***Abstract*— In this paper we derive a minimum time convergent bilateral observer for a 2×2 system of linear coupled first-order 1-D hyperbolic PDEs. First, a Volterra integral transformation is combined with a Fredholm integral transformation to derive a minimum time collocated observer for a class of $2+2$ systems (four coupled PDEs). Then, it is shown that the 2×2 system (two coupled PDEs) can be transformed to a $2+2$ system via an invertible coordinate transformation. The 2×2 bilateral observer is subsequently obtained from the $2+2$ minimum time collocated observer, and it is shown that it has convergence time equal to the theoretical minimum time for bilateral sensing. The performance of the 2×2 bilateral observer is demonstrated in a simulation and compared to a previously derived observer using only unilateral sensing.**

I. INTRODUCTION

A. Problem statement

We are interested in systems with dynamics, in terms of the state (u,v), given by

$$u_t(x,t) + \lambda(x)u_x(x,t) = \sigma^+(x)v(x,t) \tag{1a}$$
$$v_t(x,t) - \mu(x)v_x(x,t) = \sigma^-(x)u(x,t) \tag{1b}$$
$$u(0,t) = qv(0,t) + U_1(t) \tag{1c}$$
$$v(1,t) = \rho u(1,t) + U_2(t), \tag{1d}$$

defined over $x \in [0,1]$ and $t \in [0,\infty)$, where

$$\lambda, \mu \in C^1(0,1), \lambda(x), \mu(x) > 0, \forall x \in (0,1), \tag{2}$$

$\sigma^+, \sigma^- \in C^0(0,1)$, $q, \rho \in \mathbb{R}$, and $U_1(t)$ and $U_2(t)$ are boundary control inputs. We assume that the initial conditions $u(x,0) = u_0(x)$ and $v(x,0) = v_0(x)$ satisfy $u_0, v_0 \in L_2(0,1)$.

System (1) is referred to as a 2×2 hyperbolic system, and u and v are scalar values that carry information in opposite directions on $(0,1)$. More generally, u and v may be vector-valued with n and m components, respectively, in which case the system is referred to an $n+m$ hyperbolic system. Notice that 2×2 systems and $1 + 1$ systems are the same.

We assume that measurements from (1) are taken at the boundaries, only, defined as

$$y_1(t) = u(1,t) \tag{3a}$$
$$y_2(t) = v(0,t). \tag{3b}$$

The goal of the paper is to design an observer for (1), using the measurements (3), only, that provides state estimates $\hat{u}$, $\hat{v}$ which converge to the correct system states in the minimum time for bilateral sensing, defined in [1] as

$$t_{2,min} = \max\left\{ \int_0^1 \frac{dx}{\lambda(x)}, \int_0^1 \frac{dx}{\mu(x)} \right\}, \tag{4}$$

which is strictly smaller than the theoretical lower boundary $t_{1,min}$ when only measuring a single boundary, also defined in [1] as

$$t_{1,min} = \int_0^1 \frac{dx}{\lambda(x)} + \int_0^1 \frac{dx}{\mu(x)}. \tag{5}$$

In [2], the problem is solved for a general $n+m$ system, and the bilateral minimum time observer for (1), that is the $n = m = 1$ case, takes the form

$$\begin{aligned}\hat{u}_t(x,t) + \lambda(x)\hat{u}_x(x,t) = \sigma^+(x)\hat{v}(x,t) &\\ + P^{++}(x)(y_1(t) - \hat{u}(1,t)) &\\ + P^{+-}(x)(y_2(t) - \hat{v}(0,t)) &\end{aligned} \tag{6a}$$
$$\begin{aligned}\hat{v}_t(x,t) - \mu(x)\hat{v}_x(x,t) = \sigma^-(x)\hat{u}(x,t) &\\ + P^{-+}(x)(y_1(t) - \hat{u}(1,t)) &\\ + P^{--}(x)(y_2(t) - \hat{v}(0,t)) &\end{aligned} \tag{6b}$$
$$\hat{u}(0,t) = qy_2(t) + U_1(t) \tag{6c}$$
$$\hat{v}(1,t) = \rho y_1(t) + U_2(t), \tag{6d}$$

where P^{++}, P^{+-}, P^{-+} and P^{--} are observer gains tailored to achieve convergence in finite time given by (4). The initial conditions of the observer $\hat{u}(x,0) = \hat{u}_0(x)$ and $\hat{v}(x,0) = \hat{v}_0(x)$ are assumed to satisfy $\hat{u}_0, \hat{v}_0 \in L_2(0,1)$.

The contribution of the present paper is twofold: First, we design a minimum time convergent observer for a class of $2+2$ systems using a single measurement taken at one boundary. This problem has to the best of the authors' knowledge not been solved before. Second, we show that the $2+2$ system can be transformed by an invertible change of coordinates into the 2×2 system (1), thereby obtaining the observer gains in (6) by an alternative route.

To facilitate the design of the observer for the $2+2$ system, we impose the following assumption on the transport speeds of (1), in addition to (2):

$$\mu(x) \leq \overline{\mu} \leq \underline{\lambda} \leq \lambda(x), \forall x \in (0,1). \tag{7}$$

Notice that the direction of the inequality signs in (7) is chosen without loss of generality in view of the symmetry in (1). In [2], constant transport speeds are considered, so there (7) holds trivially. One immediate consequence of (7)

The authors are with the Department of Engineering Cybernetics, Norwegian University of Science and Technology, Trondheim N-7491, Norway. (e-mail: ncw@aweco.no, henrik.anfinsen@ntnu.no, aamo@ntnu.no)

is that

$$t_{2,min} = \int_0^1 \frac{dx}{\mu(x)}. \tag{8}$$

B. Background

Systems of coupled first-order linear hyperbolic PDEs, along with their observation and control problems, have been subject to research recently due to their application in modeling various physical scenarios. Applications include heat exchangers [3], gas pipelines [4] and oil well drilling [5], to name a few.

A gradually more common method for observer and controller design for this type of systems is the infinite dimensional backstepping method, initially pioneered for parabolic PDE control design in [6], and subsequently appearing in its fully infinite dimensional form in [7]. Applying the backstepping method for observer design was first seen for parabolic PDEs in [8].

In [9], the first observer for 2×2 systems (1) relying on the single boundary measurement (3a), only, was presented. An observer with single boundary sensing for the more general class of $n+m$ hyperbolic systems was achieved in [10], albeit converging in non-minimum time. The $2+2$ system observer designed in the present paper builds on the $n+m$ system observer from [10] by modifying the non-minimum time target system used there with the help of a Fredholm integral transformation, following ideas from [11], [12]. We find expressions for the 2×2 bilateral observer gains using a domain folding trick similar to the one suggested in [13] for stabilization of systems of reaction-diffusion equations, and demonstrate in simulations that our 2×2 bilateral observer converges within (8), which is quicker than (5) achieved by the observer from [9].

This paper is organized as follows. Section II presents the minimum time collocated observer design for the $2+2$ system, and the result is applied in Section III to obtain the minimum time 2×2 bilateral observer. Results from a simulation are given in Section IV before some concluding remarks are offered in Section V.

II. MINIMUM-TIME COLLOCATED OBSERVER FOR $2+2$ SYSTEMS

A. Class of $2+2$ systems

Consider now the $2+2$ system defined as

$$\bar{u}_t(x,t) + \Lambda^+(x)\bar{u}_x(x,t) = \Sigma^{+-}(x)\bar{v}(x,t) \tag{9a}$$
$$\bar{v}_t(x,t) - \Lambda^-(x)\bar{v}_x(x,t) = \Sigma^{-+}(x)\bar{u}(x,t) \tag{9b}$$
$$\bar{u}(0,t) = Q_0\bar{v}(0,t) \tag{9c}$$
$$\bar{v}(1,t) = R_1\bar{u}(1,t) + U(t), \tag{9d}$$

evolving over $x\in[0,1]$ and $t\in[0,\infty)$, where

$$\bar{u}(x,t) = [u_1(x,t), u_2(x,t)]^T \tag{10a}$$
$$\bar{v}(x,t) = [v_1(x,t), v_2(x,t)]^T \tag{10b}$$

are the states. We assume that initial conditions, defined as $\bar{u}(x,0) = [u_{1,0}(x), u_{2,0}(x)]^T$ and $\bar{v}(x,0) = [v_{1,0}(x), v_{2,0}(x)]^T$ satisfy $u_{1,0}, u_{2,0}, v_{1,0}, v_{2,0} \in L_2(0,1)$. The transport speed matrices, which are defined as

$$\Lambda^+(x) = \text{diag}\{\lambda_1(x), \lambda_2(x)\} \tag{11a}$$
$$\Lambda^-(x) = \text{diag}\{\mu_1(x), \mu_2(x)\}, \tag{11b}$$

have components satisfying $\lambda_1, \lambda_2, \mu_1, \mu_2 \in C^1(0,1)$ and are $\forall x\in(0,1)$ subject to the restriction

$$\lambda_2(x) \geq \lambda_1(x) > 0 > -\mu_1(x) \geq -\mu_2(x). \tag{12}$$

The two coupling coefficient matrices

$$\Sigma^{+-}(\bar{x}) = \{\sigma_{ij}^{+-}(\bar{x})\}_{1\leq i,j\leq 2} \tag{13a}$$
$$\Sigma^{-+}(\bar{x}) = \{\sigma_{ij}^{-+}(\bar{x})\}_{1\leq i,j\leq 2}, \tag{13b}$$

have components satisfying $\sigma_{ij}^{+-}, \sigma_{ij}^{-+} \in C^0([0,1])$, $\forall i,j\in\{1,2\}$, whereas the reflection coefficients

$$Q_0 = \{q_{ij}\}_{1\leq i,j\leq 2} \tag{14a}$$
$$R_1 = \{\rho_{ij}\}_{1\leq i,j\leq 2}, \tag{14b}$$

have $\forall i,j\in\{1,2\}$ components satisfying $q_{ij}, \rho_{ij}\in\mathbb{R}$. The term $U(t) = [U_1(t), U_2(t)]^T$ is a boundary control input for (9), entering at $x=1$. In addition to right boundary actuation, it is assumed that the collocated boundary measurement vector $y = [y_1, y_2]^T$ with components

$$y_1(t) = u_1(1,t) \tag{15a}$$
$$y_2(t) = u_2(1,t), \tag{15b}$$

is available.

B. Collocated observer for the $2+2$ system

We consider here the observer

$$\begin{aligned}\check{u}_t(x,t) + \Lambda^+(x)\check{u}_x(x,t) = \Sigma^{+-}(x)\check{v}(x,t) \\ + P^+(x)(y(t) - \check{u}(1,t))\end{aligned} \tag{16a}$$
$$\begin{aligned}\check{v}_t(x,t) - \Lambda^-(x)\check{v}_x(x,t) = \Sigma^{-+}(x)\check{u}(x,t) \\ + P^-(x)(y(t) - \check{u}(1,t)\end{aligned} \tag{16b}$$
$$\check{u}(0,t) = Q_1\check{v}(0,t) \tag{16c}$$
$$\check{v}(1,t) = R_1 y(t) + U(t) \tag{16d}$$

providing state estimates $\check{u} = [\check{u}_1, \check{u}_2]^T$ and $\check{v} = [\check{v}_1, \check{v}_2]^T$, where

$$P^+(x) = M(x,1)\Lambda^+(1) + T^+(x) + \int_x^1 M(x,\xi)T^+(\xi)d\xi, \tag{17a}$$

$$P^-(x) = N(x,1)\Lambda^+(1) + \int_x^1 N(x,\xi)T^+(\xi)d\xi, \tag{17b}$$

are the observer gains. The initial conditions for the observer (16), denoted $\check{u}(x,0) = [\check{u}_{1,0}(x), \check{u}_{2,0}(x)]^T$ and $\check{v}(x,0) = [\check{v}_{1,0}(x), \check{v}_{2,0}(x)]^T$ are assumed to satisfy $\check{u}_{1,0}, \check{u}_{2,0}, \check{v}_{1,0}, \check{v}_{2,0}\in L_2(0,1)$. M and N in (17) are 2×2 matrix-valued functions

$$M(x,\xi) = \{M_{ij}(x,\xi)\}_{1\leq i,j\leq 2} \tag{18a}$$

$$N(x,\xi) = \{N_{ij}(x,\xi)\}_{1\le i,j\le 2} \tag{18b}$$

which are solutions to the kernel PDE

$$\begin{aligned}\Lambda^+(x)M_x(x,\xi) + M_\xi(x,\xi)\Lambda^+(\xi) = -M(x,\xi)\Lambda^+_\xi(\xi)\\ + \Sigma^{+-}(x)N(x,\xi)\end{aligned} \tag{19a}$$

$$\begin{aligned}-\Lambda^-(x)N_x(x,\xi) + N_\xi(x,\xi)\Lambda^+(\xi) = -N(x,\xi)\Lambda^+_\xi(\xi)\\ + \Sigma^{-+}(x)M(x,\xi)\end{aligned} \tag{19b}$$

$$\Lambda^-(x)N(x,x) + N(x,x)\Lambda^+(x) = \Sigma^{-+}(x) \tag{19c}$$

$$Q_0N(0,\xi) - M(0,\xi) = H(\xi), \tag{19d}$$

$$M_{12}(x,x) = M_{21}(x,x) = 0 \tag{19e}$$

$$M_{21}(x,1) = 0, \tag{19f}$$

defined over the triangular domain $\mathcal{T}_u = \{(x,\xi) \mid 0 \le x \le \xi \le 1\}$. In (19d), $H = \{h_{ij}\}_{1\le i,j\le 2}$ is a strictly lower triangular 2×2 matrix, and its only non-zero component h_{21} is defined as

$$h_{21}(\xi) = \sum_{k=1}^{2} q_{2k}N_{k1}(0,\xi) - M_{21}(0,\xi). \tag{20}$$

The term $T^+ = \{T^+_{ij}\}_{1\le i,j\le 2}$ appearing in (17) is a strictly lower triangular 2×2 matrix, and its only non-zero term T^+_{21} is defined as

$$T^+_{21}(x) = k_{21}(x,1)\lambda_1(1), \tag{21}$$

where k_{21} is the solution to the PDE

$$k_{21,x}(x,\xi)\lambda_2(x) + k_{21,\xi}(x,\xi)\lambda_1(\xi) = -k_{21}(x,\xi)\lambda_{1,\xi}(\xi) \tag{22a}$$

$$k_{21}(0,\xi) = h_{21}(\xi) \tag{22b}$$

$$k_{21}(x,0) = 0. \tag{22c}$$

Provided that (12) holds, well-posedness of (19)–(20) is ensured by Theorem 3.2 in [14] whereas in [11] the explicit solution to an equation of the form (22) is given. Note that in [14] the well-posedness proof is given for the case of constant transport velocities, but it is claimed that the proof extends to cases involving spatially varying transport speeds. Next, we present a convergence result for the observer (16).

Theorem 2.1: Consider system (9) with outputs (15) and the observer (16). If the output injection gains are selected as (17)–(22), then $\check{u}(x,t)$ and $\check{v}(x,t)$ converge to $\bar{u}(x,t)$ and $\bar{v}(x,t)$, respectively, in finite time given by

$$t_{min} = \int_0^1 \frac{dx}{\mu_1(x)} + \int_0^1 \frac{dx}{\lambda_1(x)}. \tag{23}$$

Subsections II-C and II-D are devoted to proving Theorem 2.1.

C. Volterra backstepping transformation

Define the estimation errors $\tilde{u} = \bar{u} - \check{u}$ and $\tilde{v} = \bar{v} - \check{v}$. The error dynamics can then be found from (9) and (16) as

$$\begin{aligned}\tilde{u}_t(x,t) + \Lambda^+(x)\tilde{u}_x(x,t) = \Sigma^{+-}(x)\tilde{v}(x,t)\\ - P^+(x)\tilde{u}(1,t)\end{aligned} \tag{24a}$$

$$\begin{aligned}\tilde{v}_t(x,t) - \Lambda^-(x)\tilde{v}_x(x,t) = \Sigma^{-+}(x)\tilde{u}(x,t)\\ - P^-(x)\tilde{u}(1,t)\end{aligned} \tag{24b}$$

$$\tilde{u}(0,t) = Q_0\tilde{v}(0,t) \tag{24c}$$

$$\tilde{v}(1,t) = 0. \tag{24d}$$

with initial conditions are given by $\tilde{u}(x,0) = [\bar{u}_{1,0}(x) - \check{u}_{1,0}(x), \bar{u}_{2,0}(x) - \check{u}_{2,0}(x)]^T$ and $\tilde{v}(x,0) = [\bar{v}_{1,0}(x) - \check{v}_{1,0}(x), \bar{v}_{2,0}(x) - \check{v}_{2,0}(x)]^T$.

The proof of the following Lemma follows similar steps as the proof of Lemma 10 in [10], but is included here to show the details behind the new observer gains (17), which are different from those in [10] to accommodate minimum time convergence.

Lemma 2.2: The invertible Volterra integral transformation

$$\tilde{u}(x,t) = \tilde{\alpha}(x,t) + \int_x^1 M(x,\xi)\tilde{\alpha}(\xi,t)d\xi, \tag{25a}$$

$$\tilde{v}(x,t) = \tilde{\beta}(x,t) + \int_x^1 N(x,\xi)\tilde{\alpha}(\xi,t)d\xi \tag{25b}$$

maps

$$\begin{aligned}&\tilde{\alpha}_t(x,t) + \Lambda^+(x)\tilde{\alpha}_x(x,t) = \Sigma^{+-}(x)\tilde{\beta}(x,t)\\ &- \int_x^1 D^+(x,\xi)\tilde{\beta}(\xi,t)d\xi - T^+(x)\tilde{\alpha}(1,t)\end{aligned} \tag{26a}$$

$$\tilde{\beta}_t(x,t) - \Lambda^-(x)\tilde{\beta}_x(x,t) = -\int_x^1 D^-(x,\xi)\tilde{\beta}(\xi,t)d\xi \tag{26b}$$

$$\tilde{\alpha}(0,t) - Q_0\tilde{\beta}(0,t) = \int_0^1 H(\xi)\tilde{\alpha}(\xi,t)d\xi \tag{26c}$$

$$\tilde{\beta}(1,t) = 0, \tag{26d}$$

with initial conditions $\tilde{\alpha}(x,0) = [\tilde{\alpha}_{1,0}(x), \tilde{\alpha}_{2,0}(x)]^T$ and $\tilde{\beta}(x,0) = [\tilde{\beta}_{1,0}(x), \tilde{\beta}_{2,0}(x)]^T$ where $\tilde{\alpha}_{1,0}, \tilde{\alpha}_{2,0}, \tilde{\beta}_{1,0}, \tilde{\beta}_{2,0} \in L_2(0,1)$, into (24), where M and N satisfy (19)–(20). $D^+ = \{d^+_{ij}\}_{i,j\in\{1,2\}}$, $D^- = \{d^-_{ij}\}_{i,j\in\{1,2\}}$ are the solutions to the integral equations

$$\begin{aligned}D^+(x,\xi) = M(x,\xi)\Sigma^{+-}(\xi)\\ - \int_\xi^x M(\xi,s)D^+(s,\xi)ds\end{aligned} \tag{27a}$$

$$\begin{aligned}D^-(x,\xi) = N(x,\xi)\Sigma^{+-}(\xi)\\ - \int_\xi^x N(\xi,s)D^+(s,\xi)ds,\end{aligned} \tag{27b}$$

respectively.

Proof: Differentiating (25) with respect to time and space, substituting in the target error system (26), integrating by parts and combining with (24) we find

$$\begin{aligned}
&\tilde{u}_t(x,t) + \Lambda^+(x)\tilde{u}_x(x,t) - \Sigma^{+-}(x)\tilde{v}(x,t) + P^+(x)\tilde{u}(1,t) \\
&\quad = [M(x,x)\Lambda^+(x) - \Lambda^+(x)M(x,x)]\tilde{\alpha}(x,t) \\
&+ \int_x^1 [M_\xi(x,\xi)\Lambda^+(\xi) + M(x,\xi)\Lambda^+_\xi(\xi) + \Lambda^+(x)M_x(x,\xi) \\
&\quad -\Sigma^{+-}(x)N(x,\xi)]\tilde{\alpha}(\xi,t)d\xi + \int_x^1 [M(x,\xi)\Sigma^{+-}(\xi) \\
&\quad -D^+(x,\xi) - \int_\xi^x M(\xi,s)D^+(s,\xi)ds]\tilde{\beta}(\xi,t)d\xi \\
&\quad +[P^+(x) - M(x,1)\Lambda^+(1) - T^+(x) \\
&\quad - \int_x^1 M(x,\xi)T^+(\xi)d\xi]\tilde{\alpha}(1,t) = 0,
\end{aligned} \tag{28}$$

and

$$\begin{aligned}
&\tilde{v}_t(x,t) - \Lambda^-(x)\tilde{v}_x(x,t) - \Sigma^{-+}(x)\tilde{u}(x,t) + P^-(x)\tilde{u}(1,t) \\
&\quad = [N(x,x)\Lambda^+(x) + \Lambda^-(x)N(x,x) - \Sigma^{-+}(x)]\tilde{\alpha}(x,t) \\
&+ \int_x^1 [N_\xi(x,\xi)\Lambda^+(\xi) + N(x,\xi)\Lambda^+_\xi(\xi) - \Lambda^-(x)N_x(x,\xi) \\
&\quad -\Sigma^{-+}(x)M(x,\xi)]\tilde{\alpha}(\xi,t)d\xi + \int_x^1 [N(x,\xi)\Sigma^{+-}(\xi) \\
&\quad -D^-(x,\xi) - \int_\xi^x N(\xi,s)D^+(s,\xi)ds]\tilde{\beta}(\xi,t)d\xi \\
&\quad +[P^-(x) - N(x,1)\Lambda^+(1) \\
&\quad - \int_x^1 N(x,\xi)T^+(\xi)d\xi]\tilde{\alpha}(1,t) = 0.
\end{aligned} \tag{29}$$

From (28) and (29) we obtain (17), the definitions of D^+ and D^- (27), the PDE (19b) and the first two boundary conditions (19e) and (19c). For the third boundary condition (19d), set $x = 0$ in (25) and substitute this into (24c), and then apply (26c) to obtain

$$\int_0^1 H(\xi)\tilde{\alpha}(\xi,t)d\xi = \int_0^1 [Q_0N(0,\xi) - M(0,\xi)]\tilde{\alpha}(\xi,t)d\xi \tag{30}$$

from which the required boundary condition (19d) trivially follows. Finally, (19f) is an additional boundary condition required for well-posedness, as was done in [14] for equations in the same form. ∎

D. Fredholm integral transformation

Now a target system which converges in minimum time (23) is introduced, and proved to be equivalent with (26). The proof of the following Lemma relies on similar steps as in the proof of Lemma 11 in [10] together with straightforward application of the method of characteristics, but is included here for completeness.

Lemma 2.3: Consider the error system with states $\tilde{\gamma} = [\tilde{\gamma}_1, \tilde{\gamma}_2]^T$ and $\tilde{\nu} = [\tilde{\nu}_1, \tilde{\nu}_2]^T$, governed by the dynamics

$$\begin{aligned}
&\tilde{\gamma}_t(x,t) + \Lambda^+(x)\tilde{\gamma}_x(x,t) = \Sigma^{+-}(x)\tilde{\nu}(x,t) \\
&\quad - \int_x^1 D^+(x,\xi)\tilde{\nu}(\xi,t)d\xi - \int_0^1 \breve{K}_1(x,\xi)\Big(\breve{\Sigma}^{+-}(\xi)\tilde{\nu}(\xi,t) \\
&\qquad - \int_\xi^1 \breve{D}^+(\xi,s)\tilde{\nu}(s,t)ds\Big)d\xi
\end{aligned} \tag{31a}$$

$$\tilde{\nu}_t(x,t) - \Lambda^-(x,t)\tilde{\nu}_x(x,t) = -\int_x^1 D^-(x,\xi)\tilde{\nu}(\xi,t)d\xi \tag{31b}$$

$$\tilde{\gamma}(0,t) = Q_0\tilde{\nu}(0,t) \tag{31c}$$

$$\tilde{\nu}(1,t) = 0, \tag{31d}$$

and initial conditions $\tilde{\nu}(x,0) = [\tilde{\nu}_{1,0}(x), \tilde{\nu}_{2,0}(x)]^T$ and $\tilde{\gamma}(x,0) = [\tilde{\gamma}_{1,0}(x), \tilde{\gamma}_{2,0}(x)]^T$ assumed to satisfy $\tilde{\nu}_{1,0}, \tilde{\nu}_{2,0}, \tilde{\gamma}_{1,0}, \tilde{\gamma}_{2,0} \in L_2(0,1)$. Here $\breve{K}_1$, $\breve{\Sigma}^{+-}$ and $\breve{D}^+$ in (31a) are defined as

$$\breve{K}_1(x,\xi) = \begin{bmatrix} 0 & 0 \\ 0 & k_{21}(x,\xi) \end{bmatrix} \tag{32a}$$

$$\breve{\Sigma}^{+-}(x) = \begin{bmatrix} 0 & 0 \\ \sigma^{+-}_{11}(x) & \sigma^{+-}_{12}(x) \end{bmatrix} \tag{32b}$$

$$\breve{D}^+(x,\xi) = \begin{bmatrix} 0 & 0 \\ d^+_{11}(x,\xi) & d^+_{12}(x,\xi) \end{bmatrix}. \tag{32c}$$

Then $\tilde{\gamma}(x,t), \tilde{\nu}(x,t)$ converge to zero in finite time given by (23).

Proof: By the method of characteristics and cascade structure of (31), we see from (31b) with boundary (31d) that $\tilde{\nu}(x,t) \equiv 0\ \forall t \geq \int_0^1 \frac{dx}{\mu_1(x)}$. The dynamics (31a) reduces after this to $\tilde{\gamma}_t + \Lambda^+\tilde{\gamma}_x = 0$ with boundary condition $\tilde{\gamma}(0,t) = 0$, which vanishes after another $\int_0^1 \frac{dx}{\lambda_1(x)}$ time steps. ∎

We will now consider the Fredholm integral transformation

$$\tilde{\alpha}(x,t) = \tilde{\gamma}(x,t) + \int_0^1 K_1(x,\xi)\tilde{\gamma}(\xi,t)d\xi \tag{33a}$$

$$\tilde{\beta}(x,t) = \tilde{\nu}(x,t) \tag{33b}$$

with $K_1 = \{k_{ij}\}_{i,j\in\{1,2\}}$ being a strictly lower triangular 2×2 matrix, with k_{21} being the only nonzero element. We know from [11] that since K_1 is strictly lower triangular, the Fredholm integral transformation (33) is invertible.

Lemma 2.4: If k_{21} satisfies (22), then the invertible Fredholm integral transformation (33) maps the error system (31) into (26).

Proof: Noticing that (33b) is the identity, and that the first component of $\tilde{\alpha}$ equals the first component of $\tilde{\gamma}$ due to the structure of K_1, we only need to deal with the second component of $\tilde{\alpha}$, $\tilde{\alpha}_2$. Differentiating $\tilde{\alpha}_2$ in (33a) with respect to time and space, substituting in (31a), integrating by parts and combining with (26a) we find that

$$0 = \tilde{\alpha}_{2,t}(x,t) + \lambda_2(x)\tilde{\alpha}_{2,x}(x,t) - \sigma_{21}^{+-}(x)\tilde{\beta}_1(x,t)$$
$$-\sigma_{22}^{+-}(x)\tilde{\beta}_2(x,t) = [T_{21}^{+}(x) - k_{21}(x,1)\lambda_1(1)]\tilde{\gamma}_1(1,t)$$
$$+\int_0^1 [k_{21,x}(x,\xi)\lambda_2(x) + k_{21,\xi}(x,\xi)\lambda_1(\xi)$$
$$+k_{21}(x,\xi)\lambda_{1,\xi}(\xi)]\tilde{\gamma}_1(\xi,t)d\xi + k_{21}(x,0)\lambda_1(0)\tilde{\gamma}_1(0,t), \tag{34}$$

where (21)–(22) were used in the last step. Setting $x = 0$ into (33a), and comparing with (26c) we find

$$\int_0^1 K_1(0,\xi)\tilde{\gamma}(\xi,t)d\xi = \int_0^1 H(\xi)\tilde{\alpha}(\xi,t)d\xi \tag{35}$$

due to the boundary condition (22b), and the fact that $\tilde{\alpha}_1 = \tilde{\gamma}_1$. ■

We can now prove Theorem 2.1 by combining the Lemmas.

Proof: [Proof of Theorem 2.1] By Lemma 2.2 and Lemma 2.4, the dynamics of (24) and (31) are equivalent. Since by Lemma 2.3, $(\tilde{\gamma}, \tilde{\beta}) = 0$ in finite time given by (23), it follows (see (33) and (25)), that $(\tilde{u}, \tilde{v}) = 0$ in finite time given by (23). ■

III. MINIMUM-TIME BILATERAL OBSERVER FOR 2×2 SYSTEMS

A. Folding the 2×2 system into the $2 + 2$ system

Lemma 3.1: Let the transformation $T : (L_2([0,1]))^2 \mapsto (L_2([0,1]))^4$ be defined by

$$T[u,v](x) = (\begin{bmatrix} v(\frac{1}{2}(1-x)) \\ u(\frac{1}{2}(1+x)) \end{bmatrix}, \begin{bmatrix} v(\frac{1}{2}(1+x)) \\ u(\frac{1}{2}(1-x)) \end{bmatrix}) \tag{36}$$

with inverse $T^{-1} : (L_2([0,1]))^4 \mapsto (L_2([0,1]))^2$ given by

$$T^{-1}[\bar{u},\bar{v}](x) = \begin{cases} (v_2(1-2x), u_1(1-2x)), & x \in [0, \frac{1}{2}] \\ (u_2(2x-1), v_1(2x-1)), & x \in (\frac{1}{2}, 1] \end{cases}. \tag{37}$$

The invertible change of coordinates $(\bar{u}(x,t), \bar{v}(x,t)) = T[u,v](x,t)$ maps (1) into (9), with coefficients given by

$$\Lambda^+(x) = \begin{bmatrix} 2\mu(\frac{1}{2}(1-x)) & 0 \\ 0 & 2\lambda(\frac{1}{2}(1+x)) \end{bmatrix} \tag{38a}$$

$$\Lambda^-(x) = \begin{bmatrix} 2\mu(\frac{1}{2}(1+x)) & 0 \\ 0 & 2\lambda(\frac{1}{2}(1-x)) \end{bmatrix} \tag{38b}$$

$$\Sigma^{+-}(x) = \begin{bmatrix} 0 & \sigma^-(\frac{1}{2}(1-x)) \\ \sigma^+(\frac{1}{2}(1+x)) & 0 \end{bmatrix} \tag{38c}$$

$$\Sigma^{-+}(x) = \begin{bmatrix} 0 & \sigma^-(\frac{1}{2}(1+x)) \\ \sigma^+(\frac{1}{2}(1-x)) & 0 \end{bmatrix}, \tag{38d}$$

$$Q_0 = \begin{bmatrix} 1 & 0 \\ 0 & 1 \end{bmatrix}, \qquad R_1 = \begin{bmatrix} 0 & \rho \\ q & 0 \end{bmatrix} \tag{39a}$$

$$U(t) = \begin{bmatrix} U_2(t) \\ U_1(t) \end{bmatrix}, \qquad y(t) = \begin{bmatrix} y_2(t) \\ y_1(t) \end{bmatrix}. \tag{39b}$$

Proof: Differentiating (36) with respect to x and applying the chain rule we can express $\bar{u}_x$ and $\bar{v}_x$ in terms of u_x and v_x as

$$\bar{u}_x(x,t) = \begin{bmatrix} -\frac{1}{2}v_x(\frac{1}{2}(1-x),t) \\ \frac{1}{2}u_x(\frac{1}{2}(1+x),t) \end{bmatrix} \tag{40a}$$

$$\bar{v}_x(x,t) = \begin{bmatrix} \frac{1}{2}v_x(\frac{1}{2}(1+x),t) \\ -\frac{1}{2}u_x(\frac{1}{2}(1-x),t) \end{bmatrix}. \tag{40b}$$

Also, differentiating (36) with respect to time, we find

$$\bar{u}_t(x,t) = \begin{bmatrix} v_t(\frac{1}{2}(1-x),t) \\ u_t(\frac{1}{2}(1+x),t) \end{bmatrix} \tag{41a}$$

$$\bar{v}_t(x,t) = \begin{bmatrix} v_t(\frac{1}{2}(1+x),t) \\ u_t(\frac{1}{2}(1-x),t) \end{bmatrix}. \tag{41b}$$

Inserting (40) and (41) into (9) and comparing to (1) we find that the transport speeds can be assigned as (38a)–(38b) and the coupling coefficients become (38c)–(38d). In order to obey the restriction (12) which is a prerequisite for well-posedness of (19), we must have

$$\lambda(\frac{1}{2}(1+x)) \geq \mu(\frac{1}{2}(1-x)) \tag{42a}$$

$$\lambda(\frac{1}{2}(1-x)) \geq \mu(\frac{1}{2}(1+x)) \tag{42b}$$

which trivially satisfies (7) $\forall x \in [0,1]$. Applying (36) for $x = 0$ and $x = 1$ we find

$$\bar{u}(0,t) = \begin{bmatrix} v(\frac{1}{2},t) \\ u(\frac{1}{2},t) \end{bmatrix}, \qquad \bar{v}(0,t) = \begin{bmatrix} v(\frac{1}{2},t) \\ u(\frac{1}{2},t) \end{bmatrix} \tag{43a}$$

$$\bar{u}(1,t) = \begin{bmatrix} v(0,t) \\ u(1,t) \end{bmatrix}, \qquad \bar{v}(1,t) = \begin{bmatrix} v(1,t) \\ u(0,t) \end{bmatrix} \tag{43b}$$

which confirms that the inverse transform (37) is well-defined and the boundary condition matrices along with boundary measurement and control assignments can be found as (39). ■

B. 2×2 bilateral observer with minimum time convergence

Now we find the observer gains for (6), and prove that using these it converges within time $t_{2,min}$ given by (8).

Lemma 3.2: The invertible change of coordinates $(\hat{u}(x,t), \hat{v}(x,t)) = T^{-1}[\check{u}_1, \check{u}_2, \check{v}_1, \check{v}_2](x,t)$, maps (16) into (6) with observer gains given in terms of (17) as

$$P^{++}(x) = \begin{cases} P_{22}^-(1-2x), & x \in [0, \frac{1}{2}] \\ P_{22}^+(2x-1), & x \in (\frac{1}{2}, 1] \end{cases} \tag{44a}$$

$$P^{+-}(x) = \begin{cases} P_{21}^-(1-2x), & x \in [0, \frac{1}{2}] \\ P_{21}^+(2x-1), & x \in (\frac{1}{2}, 1] \end{cases} \tag{44b}$$

$$P^{-+}(x) = \begin{cases} P_{12}^+(1-2x), & x \in [0, \frac{1}{2}] \\ P_{12}^-(2x-1), & x \in (\frac{1}{2}, 1] \end{cases} \tag{44c}$$

$$P^{--}(x) = \begin{cases} P_{11}^+(1-2x), & x \in [0, \frac{1}{2}] \\ P_{11}^-(2x-1), & x \in (\frac{1}{2}, 1] \end{cases}. \tag{44d}$$

Proof: Consider first the left half-interval $x \in [0, \frac{1}{2}]$. From (37) we have $\hat{u}(x,t) = \check{v}_2(1-2x,t)$ and $\hat{v}(x,t) = \check{u}_1(1-2x,t)$. Taking the terms for $\check{v}_2(x,t)$ and $\check{u}_1(x,t)$ from (16), applying the coefficient assignments (38)–(39) and substituting in $\hat{u}(x,t)$ and $\hat{v}(x,t)$ along with their respective partial derivatives, which are equivalent to the ones from (40)–(41), we find

$$\begin{aligned}\hat{u}_t(x,t) - 2\lambda(x)(-\frac{1}{2}\hat{u}_x(x,t)) = \sigma^+(x)\hat{v}(x,t) + \\ P_{21}^-(1-2x)(y_2(t) - \hat{v}(0,t)) + \\ P_{22}^-(1-2x)(y_1(t) - \hat{u}(1,t)),\end{aligned} \quad (45a)$$

$$\begin{aligned}\hat{v}_t(x,t) + 2\mu(x)(-\frac{1}{2}\hat{v}_x(x,t)) = \sigma^-(x)\hat{v}(x,t) + \\ P_{11}^+(1-2x)(y_2(t) - \hat{v}(0,t)) + \\ P_{12}^+(1-2x)(y_1(t) - \hat{u}(1,t)).\end{aligned} \quad (45b)$$

Comparing (45) to (6), we obtain the observer gains in (44) valid $\forall x \in [0, \frac{1}{2}]$. Applying the same steps for the right half-interval $x \in (\frac{1}{2}, 1]$, the observer gain assignments in (44) valid $\forall x \in (\frac{1}{2}, 1]$ are obtained. ■

Theorem 3.3: Consider system (1) with outputs (3) and the observer (6). If the output injection gains are selected as (44), then $\hat{u}(x,t)$ and $\hat{v}(x,t)$ converge to $u(x,t)$ and $v(x,t)$, respectively, in finite time given by (8).

Proof: From Lemma 3.2 we know that (6) is mapped into (16) using the invertible transform (36). Hence the convergence time of (6) can be expressed as (23) using the relevant transport speeds from (38a)–(38b) as

$$t_{min} = \int_0^1 \frac{d\bar{x}}{2\mu(\frac{1}{2}(1+\bar{x}))} + \int_0^1 \frac{d\bar{x}}{2\mu(\frac{1}{2}(1-\bar{x}))}. \quad (46)$$

Applying the change of variables $\bar{x} = 2x - 1$ to the first integral and $\bar{x} = 1 - 2x$ to the second integral, we find

$$\begin{aligned} t_{min} &= \int_{\frac{1}{2}}^1 \frac{2dx}{2\mu(x)} + \int_{\frac{1}{2}}^0 \frac{-2dx}{2\mu(x)} = \int_{\frac{1}{2}}^1 \frac{dx}{\mu(x)} + \int_0^{\frac{1}{2}} \frac{dx}{\mu(x)} \quad (47) \\ &= \int_0^1 \frac{dx}{\mu(x)} \end{aligned}$$

which is (8). ■

IV. SIMULATION

The 2×2 system (1) is implemented along with the bilateral observer (6) in `MATLAB` using the method presented in [15] for solving the kernel equations. The right boundary observer from [9] is also implemented for comparison. The system and observers are implemented with coefficients

$$\lambda(x) = 1, \qquad \mu(x) = \frac{1}{2} \quad (48a)$$

$$\sigma^+(x) = x^2, \qquad \sigma^-(x) = -\sin(3x) \quad (48b)$$

$$q = 1, \qquad \rho = \frac{1}{2} \quad (48c)$$

and initial conditions and inputs

$$u_0(x) = \cos(8x), \qquad v_0(x) = e^{-x} \quad (49a)$$

$$U_1(t) = \sin(t), \qquad U_2(t) = \cos(8t). \quad (49b)$$

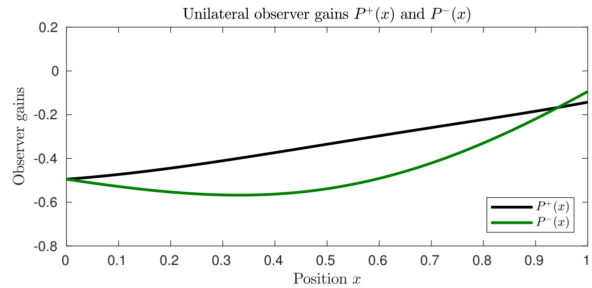

Fig. 1: Graphs of observer gains $P^+(x)$ and $P^-(x)$, $x \in (0,1)$, multiplied by $\tilde{u}(1)$ in unilateral observer.

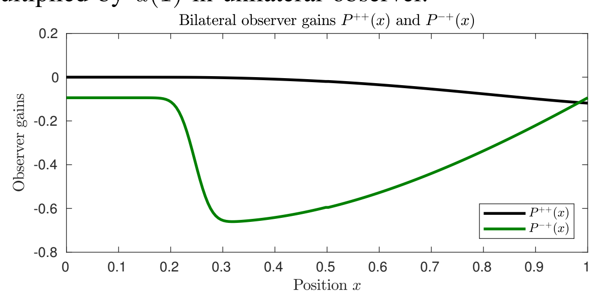

(a) Observer gains P^{++} and P^{-+} multiplied by $\tilde{u}(1)$ in bilateral observer.

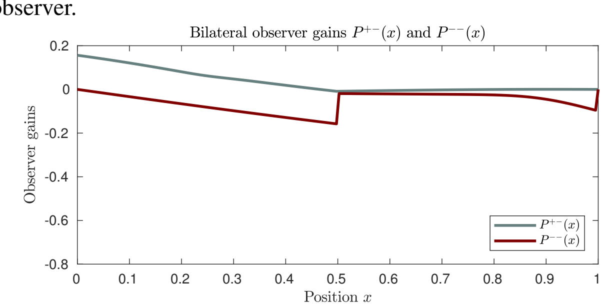

(b) Observer gains P^{+-} and P^{--} multiplied by $\tilde{v}(0)$ in bilateral observer.

Fig. 2: Graphs of observer gains $P^{++}(x)$, $P^{+-}(x)$, $P^{-+}(x)$ and $P^{--}(x)$, $x \in (0,1)$, used by bilateral observer.

The unilateral observer only uses the right boundary measurement $y_1(t) = u(1,t)$, whereas the bilateral observer additionally uses the left boundary measurement $y_2(t) = v(0,t)$. A graph of the gains $P^+(x)$ and $P^-(x)$, used by the unilateral observer to weight the measurement error $\tilde{u}(1,t)$ are shown in Fig. 1. Fig. 2 shows the gains used by the bilateral observer, for comparison, where in Fig. 2a the graphs of $P^{++}(x)$ and $P^{-+}(x)$, which weight the same measurement error $\tilde{u}(1,t)$ for the bilateral observer, are shown, whereas Fig. 2b shows the gains $P^{+-}(x)$ and $P^{--}(x)$ which weight the other measurement error $\tilde{v}(0,t)$.

Next, in Fig 3 we see the L_2-norms $||u(t)||$, $||v(t)||$ of the respective states $u(x,t)$, $v(x,t)$ of the system (1) with parameters given by (48)–(49). Hence we see that the system states do not go to zero for the duration of the simulation and the observation problem is thus nontrivial.

In Fig. 4 the norms of the estimation errors along with the theoretical convergence times are on display. Here Fig. 4a shows $||\tilde{u}(t)||$ for both observers, whereas Fig. 4b shows

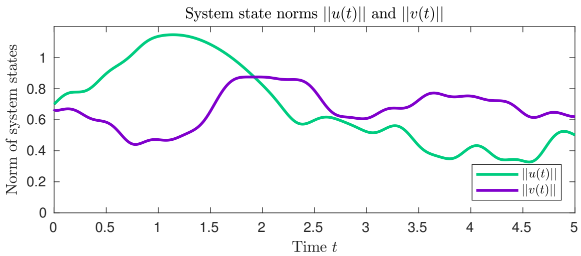

Fig. 3: Time evolution of the L_2-norms $||u(t)||$ and $||v(t)||$ of respective system states $u(x,t)$ and $v(x,t)$.

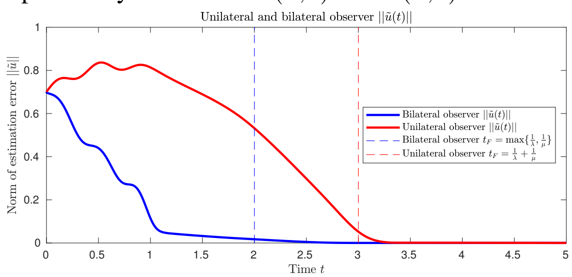

(a) Time evolution of $||\tilde{u}(t)||$.

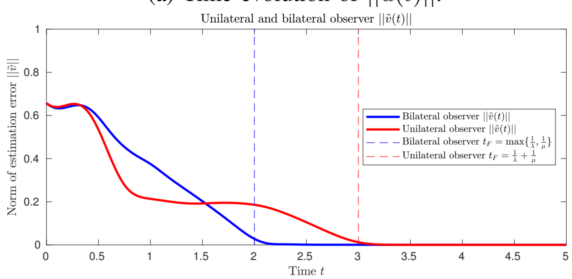

(b) Time evolution of $||\tilde{v}(t)||$.

Fig. 4: Time evolution of the L_2-norms $||\tilde{u}(t)||$, $||\tilde{v}(t)||$ of the errors $\tilde{u}(x,t)$,$\tilde{v}(x,t)$, respectively.

$||\tilde{v}(t)||$ for both observers, shown as solid lines in both plots. The theoretical convergence times t_F are represented by the dashed lines.

Note that the estimation errors associated with both the bilateral and unilateral observer have slightly non-zero values when crossing the dashed lines corresponding to their respective convergence times. This is most likely due to the first-order numerical scheme used when implementing the simulation. The theory was proven for a continuous PDE system with the observer gains expressed exactly; however in practice this ideal scenario is generally not possible to reproduce perfectly and some approximation error must be expected.

V. CONCLUSIONS

We have shown an alternative way of deriving a 2×2 minimum time bilateral observer than the one presented in [2]. An observer for (1) utilizing measurements from both boundaries was derived, going via the derivation of a minimum time collocated observer for the $2+2$ system (9), which was done by making the target system converge in minimum time with the help of a Fredholm transformation. The bilateral observer was shown to converge within the theoretical lower convergence bound from [1] for observers using both boundary measurements. As was noted in [13], some of the ideas considered there for control design could be applied to the design of bilateral observers. Indeed, this paper demonstrates that the trick of domain folding is also applicable within the venue of observation problems, and it would therefore be interesting to investigate its applicability to the design of observers for systems different from the hyperbolic ones considered here.

REFERENCES

[1] T. Li and B. Rao, "Strong (weak) exact controllability and strong (weak) exact observability for quasilinear hyperbolic systems," *Chinese Annals of Mathematics, Series B*, vol. 31, no. 5, pp. 723–742, 2010.
[2] J. Auriol and F. Di Meglio, "Two-sided boundary stabilization of heterodirectional linear coupled hyperbolic PDEs," *IEEE Transactions on Automatic Control*, vol. 63, no. 8, pp. 2421–2436, 2018.
[3] C.-Z. Xu and G. Sallet, "Exponential stability and transfer functions of processes governed by symmetric hyperbolic systems," *ESAIM: Control, Optimisation and Calculus of Variations*, vol. 7, pp. 421–442, 2002.
[4] M. Gugat, M. Dick, and G. Leugering, "Gas flow in fan-shaped networks: Classical solutions and feedback stabilization," *SIAM Journal on Control and Optimization*, vol. 49, no. 5, pp. 2101–2117, 2011.
[5] F. Di Meglio and U. J. F. Aarsnes, "A distributed parameter systems view of control problems in drilling," *IFAC-PapersOnLine*, vol. 48, no. 6, pp. 272–278, 2015.
[6] D. M. Boskovic, M. Krstic, and W. Liu, "Boundary control of an unstable heat equation via measurement of domain-averaged temperature," *IEEE Transactions on Automatic Control*, vol. 46, no. 12, pp. 2022–2028, 2001.
[7] W. Liu, "Boundary feedback stabilization of an unstable heat equation," *SIAM journal on control and optimization*, vol. 42, no. 3, pp. 1033–1043, 2003.
[8] A. Smyshlyaev and M. Krstic, "Backstepping observers for a class of parabolic PDEs," *Systems & Control Letters*, vol. 54, no. 7, pp. 613–625, 2005.
[9] R. Vazquez, M. Krstic, and J.-M. Coron, "Backstepping boundary stabilization and state estimation of a 2× 2 linear hyperbolic system," in *Decision and Control and European Control Conference (CDC-ECC), 2011 50th IEEE Conference on*. IEEE, 2011, pp. 4937–4942.
[10] H. Anfinsen and O. M. Aamo, "Disturbance rejection in general heterodirectional 1-D linear hyperbolic systems using collocated sensing and control," *Automatica*, vol. 76, pp. 230–242, 2017.
[11] J.-M. Coron, L. Hu, and G. Olive, "Finite-time boundary stabilization of general linear hyperbolic balance laws via fredholm backstepping transformation," *Automatica*, vol. 84, pp. 95–100, 2017.
[12] J. Auriol and F. Di Meglio, "Minimum time control of heterodirectional linear coupled hyperbolic PDEs," *Automatica*, vol. 71, pp. 300–307, 2016.
[13] R. Vazquez and M. Krstic, "Bilateral boundary control of one-dimensional first-and second-order PDEs using infinite-dimensional backstepping," in *Decision and Control (CDC), 2016 IEEE 55th Conference on*. IEEE, 2016, pp. 537–542.
[14] L. Hu, F. Di Meglio, R. Vazquez, and M. Krstic, "Control of homodirectional and general heterodirectional linear coupled hyperbolic PDEs," *IEEE Transactions on Automatic Control*, vol. 61, no. 11, pp. 3301–3314, 2016.
[15] H. Anfinsen and O. M. Aamo, "Adaptive stabilization of 2×2 linear hyperbolic systems with an unknown boundary parameter from collocated sensing and control," *Automatic Control, IEEE Transactions on*, vol. 62, no. 12, pp. 6237–6249, December 2017.